

Pakistan Journal of Marine Sciences, Vol. 20(1&2), 61-73, 2011.

## SYNTHESIS, CHARACTERIZATION, MOLECULAR MODELING AND ANTI-ALGAL ACTIVITIES OF A SCHIFF BASE AND ITS M<sup>+2</sup> COMPLEXES

Zahid Khan, Muhammad Asad K. Tanoli, Zahida T. Maqsood,  
Tehseen Ahmed, Majid Mumtaz

Department of Chemistry, Faculty of Science, University of Karachi,  
Karachi-75270, Pakistan .  
email: zahidyankee@gmail.com

**ABSTRACT:** In present work Four new complexes of 2-hydroxy-5-methylbenzaldehyde-N-(2-oxo-1,2-dihydro-3H-indol-3-ylidene)hydrazine have been synthesized with some transition metals, i.e. Ni<sup>+2</sup>, Cu<sup>+2</sup>, Co<sup>+2</sup> and Zn<sup>+2</sup> in non-aqueous medium. Complexes were characterized by magnetic moment, conductance, scanning electron microscopy (SEM) and spectroscopic investigations including infrared, ultraviolet-visible and atomic absorption spectroscopy. To support experimental characterization, quantum mechanical and molecular mechanical (QM/MM) calculations were performed. Experimental results with the support of QM and MM computations highlighted the proposition about the ligand to be bound to the metal ions in a tridentate manner through its phenolic oxygen, azomethine nitrogen and carbonyl group (C=O). On the basis of experimental and computational results, tetrahedral geometry is proposed for Cu<sup>+2</sup> complex and distorted tetrahedral geometry is proposed for Zn<sup>+2</sup> complex while octahedral geometries are proposed for Co<sup>+2</sup> and Ni<sup>+2</sup> complexes. For all compounds, anti-cyanobacterial (algicidal) activity was evaluated against three marine cyanobacteria i.e. *Pseudoanabaena lonchoides*, *Lyngbya contorta*, and *Spirulina major*. It was found that the metal complexes are more potent anti-cyanobacterial agents than the ligand.

**KEYWORDS:** Schiff Bases, Anti-Cyanobacterial agents, Molecular Modeling, MM/QM Calculations.

### INTRODUCTION

Marine ecosystems can be effected by harmful algal blooms (HABs) causing huge and diverse impact depending on the species involved, their environment, and the mechanism of how they cause their negative effects. A number of aquatic organisms, mainly seabirds, marine mammals, fin fishes, and sea turtles etc. have been found adversely effected by the HABs. HABs toxins can cause harmful changes to these species such as their development, immunological, neurological, and reproductive capabilities (Landsberg, 2002; Ouellette, Handy, & Wilhelm, 2006) and a number of methods have been developed including biosynthesis and biogeochemical processes to control the HABs (Hallegraeff, 1993), but very less attention have been paid to the synthetic compounds to test their anti-cyanobacterial abilities.

Schiff bases are remarkable compounds from the biological stand point and can be promising anti-cyanobacterial agents, these compounds also exhibits incredible ligational features towards transition metals as well and their coordination complexes Which are widely studied for broad range of biological applications i.e. anti-bacterial, anti-fungal,

anti-viral, anti-oxidant, anti-inflammatory, anti-glycation and anti-convulsant (El-Tabl, El-Saied, & Al-Hakimi, 2008; Khan et al., 2009; Varghese & Muraleedharan Nair, 2010).

In this research, synthesis, characterization and anti-cyanobacterial activities of Schiff base 2-hydroxy-5-methylbenzaldehyde-N-(2-oxo-1,2-dihydro-3H-indol-3-ylidene) hydrazone and its  $\text{Co}^{+2}$ ,  $\text{Ni}^{+2}$ ,  $\text{Cu}^{+2}$  and  $\text{Zn}^{+2}$  complexes have been studied. The biological activity was evaluated of all compounds against three cyanobacterial species e.g. *Pseudoanabaena lonchoides*, *Lyngbya contorta*, and *Spirulina major* in a comparative way.

Molecular modeling studies were performed for all compounds for theoretical support of the experimental data. The ligand molecule was optimized using PM3 semi-empirical method while geometries of complexes were optimized using molecular mechanics (MMFF94 force field) for faster performance. Results are well in agreement with the experimental characterizations.

Results of biological tests indicates that the complexation of the ligand increases the anti-cyanobacterial activity compared to the free ligand. The  $\text{Ni}^{+2}$  complex shows a better inhibition among all the compounds.

## MATERIALS & METHODS

All chemicals including solvents, isatin, metal salts and hydrazine hydrated were of analytical grade, purchased from Sigma-Aldrich.

**Synthesis of bis Schiff Base Ligand:** Ligand compound was synthesized by taking 2.94g of isatin and was slowly added to 20.0 mL of hydrazine hydrated solution with constant stirring in a beaker, the reaction mixture was poured into a round bottom flask containing about 50 mL hot methanol. This reaction mixture was set on a sand bath for refluxing for an hour that produced a yellow colored solid of isatin mono-hydrazone. On cooling the isatin mono-hydrazone was filtered, washed, and dried in vacuum and recrystallized using methanol.

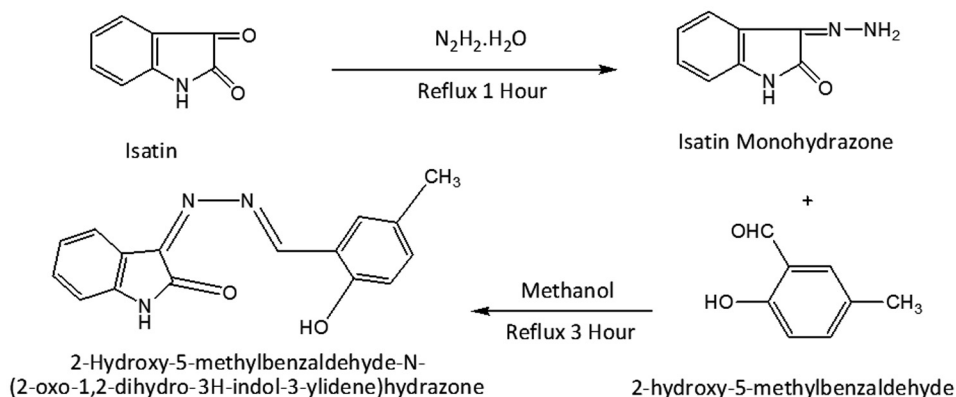


Fig.1. Synthesis of bis Schiff base

To synthesize the Schiff base ligand, equimolar solutions of 2-hydroxy-5-methylbenzaldehyde and isatin mono-hydrazone were refluxed over sand bath for three hours in methanol. As reaction proceeded the bright orange colored Schiff base started precipitating out in the flask. The progress of reaction was monitored by TLC. On completion, the flask was allowed to cool and solid product was filtered, washed, dried in vacuum and recrystallized from methanol. *Fig.1.* shows both steps of synthesis of the Schiff base.

**Synthesis of Metal Complexes:** Metal acetate salts e.g.  $\text{Co}(\text{OAc})_2 \cdot 2\text{H}_2\text{O}$ ,  $\text{Ni}(\text{OAc})_2 \cdot 4\text{H}_2\text{O}$ ,  $\text{Cu}(\text{OAc})_2 \cdot 2\text{H}_2\text{O}$  and  $\text{Zn}(\text{OAc})_2 \cdot 4\text{H}_2\text{O}$  were used to synthesize the metal complexes. For synthesizing complexes, 0.01M solution of Schiff base ligand was treated with 0.005M of metal solutions and refluxed on water bath for three hours. The solutions were subsequently concentrated and allowed to cool. The solid product that separated out on the completion of reaction was filtered, washed with hot water and ether and dried under vacuum. *Table 3.2* lists the data of physical and elemental analysis of newly synthesized complexes.

**Characterization & Physical Measurements:** Elemental analysis of complexes was performed on PerkinElmer micro analyzer 2400 series II CHN/S. Metal content was analyzed on Perkin Elmer atomic absorption spectrophotometer A-Analyst 700. The infrared spectra were recorded on Shimadzu FTIR spectrophotometer IR-Prestige-21. Electronic spectra of metal complexes were analysed on Shimadzu UV-VIS spectrophotometer UV-1601. Molar conductance values of metal complexes of  $10^{-3}\text{M}$  solutions in DMSO were measured on conductivity meter Jenway4701. Magnetic susceptibility values were measured at room temperature with a Mark 1 magnetic susceptibility balance from Sherwood Scientific. JSM 6380A scanning electron microscope from Jeol Japan was utilized for SEM pictographs. The samples were gold coated with JFC-1500 Auto Coater from Jeol Japan with gold target up to 300 Å.

**Molecular Modeling Details:** Computations were performed on an Intel Pentium 4 computer with 2.4 GHz CPU and 4.0 GB of physical memory. Argus Lab 4.0.1 software (Thompson, 2004) and Merck Force Field (MMFF94) (Halgren, 1999) were used for initial molecular modeling and geometry clean up. The geometry of Schiff base was optimized by semi-empirical PM3 Hamiltonian executed in GAMESS software package (Schmidt *et al.*, 1993). Keeping in view the large size of complexes and presence of comprehensive spectral evidences for the metal complexes, the advantage of fast performance of molecular mechanics was taken to optimize the structures of metal complexes. Results of the computations were visualized by ChemCraft version 1.6 including high resolution images of the optimized structures (Zhurko & Zhurko, 2005).

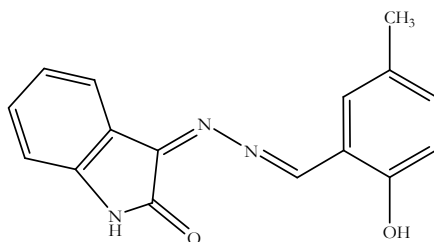
**Anti Cyanobacterial Study:** Study was performed according to American Standard Testing Method (ASTM D5589-97, 2002). Pieces of filter paper of about 1.5 mm in diameter were immersed in test solution (~0.3 mg/ml), subsequently dried and used as the substrate inhibition tests of algal growth. These test specimens were placed on a layer of solid Allen's agar in a petri dish. Three algal species i.e. *Lyngbya contorta*, *Pseudo-*

*anabaena lonchooides*, and *Spirulina major* were used for the study. Algal inoculums were aseptically transferred from the flask and a thin coat of algae suspension was applied to each specimen making sure each test specimen is covered equally with the suspension (Bravo, Héctor, 1997). The inoculated plates were set in incubator under 29°C and humidity above 85% and were examined weekly for growth inhibition up to 6 weeks.

## RESULTS & DISCUSSION

**Structure of Ligand:** Results of elemental analysis, molecular formulae, structures, IUPAC names, and some other preliminary data have been tabulated in *Table 1*. In elemental analysis, the experimental values for carbon, hydrogen, and nitrogen are written in parenthesis. The detailed spectral characterization can be found in a previous work of our research associates (Khan et al., 2009).

**Table 1. Structure & Analytical Data of Schiff Base Ligand**

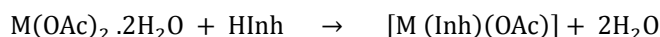


**2-hydroxy-5-methylbenzaldehyde-N-(2-oxo-1,2-dihydro-3H-indol-3-ylidene)hydrazone**

Yield	87%
Color	Orange
EI MS: m/z (rel. abund.%)	279 (M <sup>+</sup> , 48)
Molecular Formula	C <sub>16</sub> H <sub>13</sub> N <sub>3</sub> O <sub>2</sub>
Elemental Analysis	C = 68.81 (67.98), H = 04.69 (04.02), N = 15.05 (14.77)

**Structure of Complexes:** For all complexes the Schiff base acted as a tri-dentate ligand and coordinated with the metal ions through phenolic oxygen, azomethine nitrogen and carbonyl group. Physical and analytical data of complexes is presented in *Table 3.2* while *Figures 3 & 4* shows the general structures of complexes.

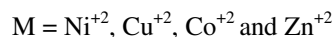
Formation of the  $\text{Cu}^{+2}$  and  $\text{Zn}^{+2}$  complexes can be presented by the following general equation.



While the formation of the complexes of  $\text{Co}^{+2}$  and  $\text{Ni}^{+2}$  can be presented by the following general equation.



Where



HInh = 2-hydroxy-5-methylbenzaldehyde-N-(2-oxo-1,2-dihydro-3H-indol-3-ylidene)hydrazone

**Table 2. Physical & Analytical Data of Complexes**

Compound with Melting Point	Molecular Formula	Formula Mass	%Yield / Color	Analytical Data*				Molar Conductance in DMSO ( $\text{ohm}^{-1} \text{cm}^2 \text{mol}^{-1}$ )	Magnetic Moment (B.M)
				M	C	H	N		
[Co(Inh) <sub>2</sub> ] M.P > 300 °C	CoC <sub>32</sub> H <sub>28</sub> N <sub>6</sub> O <sub>4</sub>	619.54	76 Green	09.51 (8.83)	62.04 (61.77)	4.56 (3.65)	13.57 (13.13)	6.3	4.86
[Ni(Inh) <sub>2</sub> ] M.P > 300 °C	NiC <sub>32</sub> H <sub>28</sub> N <sub>6</sub> O <sub>4</sub>	619.30	82 Green	9.48 (9.08)	62.06 (61.87)	4.56 (4.19)	13.57 (13.34)	6.9	3.12
[Cu(Inh)(OAc)] M.P > 300 °C	CuC <sub>18</sub> H <sub>17</sub> N <sub>3</sub> O <sub>4</sub>	402.89	70 Brown	15.77 (14.99)	53.66 (52.98)	4.25 (4.01)	10.43 (10.11)	5.5	1.82
[Zn(Inh)(OAc)] M.P > 300 °C	ZnC <sub>18</sub> H <sub>17</sub> N <sub>3</sub> O <sub>4</sub>	404.74	71 Dark Red	16.16 (15.67)	53.42 (52.97)	4.23 (3.88)	10.38 (9.79)	6.2	D

\*Calculated values are given in parentheses.

Synthesized complexes were stable, non-hygroscopic and insoluble in water but soluble in DMSO. Elemental analysis of the complexes showed that the  $\text{Cu}^{+2}$  and  $\text{Zn}^{+2}$  complexes have 1:1 metal-ligand mole ratio while complexes of  $\text{Ni}^{+2}$  and  $\text{Co}^{+2}$  have 1:2 metal-ligand mole ratios. Molar conductance data suggest the non-electrolyte nature of all complexes.

**IR Spectra of Complexes:** Infrared spectral data has been given in *Table 3*. with provisional band assignments. The broad band of hydrogen bonded OH group disappeared (at  $3381\text{cm}^{-1}$ ) in the infrared spectra of metal complexes which is an indication of the deprotonation and C–O bond formation. An increase in frequency for C–

O bonds is a clear sign of the coordination of phenolic oxygen to the metal ion. Stretching frequencies of C=Nis decreased noticeably from  $1689\text{ cm}^{-1}$  which justifies the involvement of aldimine nitrogen in the coordination. The band corresponds to C=O shifted to lower frequency in the spectra of metal complexes offering evidence for coordination by carbonyl oxygen. The vibration characteristics of the ring (NH and C=N) however, remained unaltered which indicates that these groups did not participate in the coordination.

The non-ligand peaks are appearing in the regions of  $512\text{ cm}^{-1} - 524\text{ cm}^{-1}$  and  $452\text{ cm}^{-1} - 474\text{ cm}^{-1}$  can be assigned to M-O and M-N bonds respectively. Therefore from the infrared spectra of metal complexes it is clear that the ligand coordinated to the metal ions in a tridentate fashion through the deprotonated phenolic oxygen, aldimine nitrogen and carbonyl oxygen.

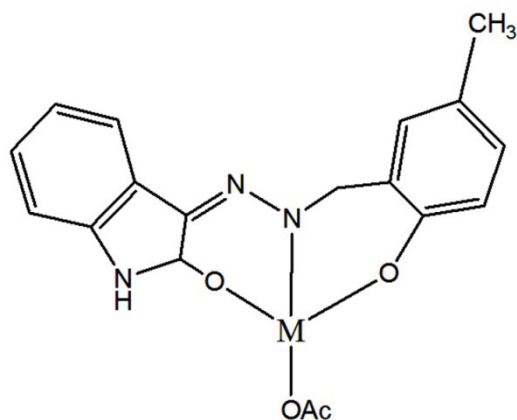


Fig. 2. General Structure of  $\text{Cu}^{+2}$  and  $\text{Zn}^{+2}$  Complexes

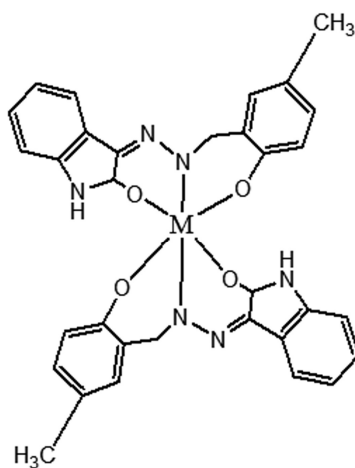


Fig. 3. General Structure of  $\text{Co}^{+2}$  and  $\text{Ni}^{+2}$  Complexes

**Table 3. Important Infrared Absorptions**

<b>HIInh</b>	<b>[ Co (Inh)<sub>2</sub> ]</b>	<b>[ Ni (Inh)<sub>2</sub> ]</b>	<b>[ Cu (Inh)(OAc) ]</b>	<b>[ Zn (Inh)(OAc) ]</b>	<b>Provisional Assignments</b>
3381mb	-	-	-	-	(OH) group
3080m	3054m	3068m	3053m	3054m	(NH)Indol ring
1715s	1672s	1680s	1682s	1685s	(C=O)
1689m	1647m	1649m	1635m	1640m	(C=N) ring
1624s	1597m	1606m	1605s	1604m	(C=N) aldimine
1355s	1378s	1377s	1376s	1369s	(C-O) phenolic
1064m	1096m	1087m	1095m	1096m	(N-N) hydrazine
-	452	467	453	474	(M-N)
-	518	512	517	524	(M-O)

**Electronic Spectra of Complexes:** Two absorption bands in between 337nm to 390nm are exhibited in the ultraviolet spectrum of ligand which can be assigned to  $n-\pi^*$  transitions of the aldimine and ketamine moieties respectively (Patel, Parekh, & Patel, 2005). Ultraviolet spectrum of  $\text{Co}^{+2}$  complex shows bands at  $29070\text{ cm}^{-1}$ ,  $20368\text{ cm}^{-1}$ ,  $93454\text{ cm}^{-1}$  corresponding to  $\nu_1$ ,  $\nu_2$  and  $\nu_3$  transitions respectively, which can be attributed to  ${}^4\text{T}_{1g}(\text{F}) \rightarrow {}^4\text{T}_{2g}(\text{F})$  ( $\nu_1$ ),  ${}^4\text{T}_{1g}(\text{F}) \rightarrow {}^4\text{A}_{2g}(\text{F})$  ( $\nu_2$ ),  ${}^4\text{T}_{1g}(\text{F}) \rightarrow {}^4\text{T}_{1g}(\text{P})$  ( $\nu_3$ ) transitions which are the characteristic for high spin octahedral  $\text{Co}^{+2}$  complex (Patel *et al.*, 2005). The magnetic moment value for  $\text{Co}^{+2}$  complex is 4.86 which is also well in agreement with the octahedral geometry.

Ultraviolet spectrum of  $\text{Ni}^{+2}$  complex shows three bands at  $28986\text{ cm}^{-1}$ ,  $19569\text{ cm}^{-1}$ , and  $10415\text{ cm}^{-1}$  which can be attributed to the  ${}^3\text{A}_{2g} \rightarrow {}^3\text{T}_{2g}$  ( $\nu_1$ ),  ${}^3\text{A}_{2g} \rightarrow {}^3\text{T}_{1g}(\text{F})$  ( $\nu_2$ ) and  ${}^3\text{A}_{2g} \rightarrow {}^3\text{T}_{1g}(\text{P})$  ( $\nu_3$ ) respectively, which is clearly indicating the octahedral geometry

around  $\text{Ni}^{+2}$  ion. Magnetic moment value of 3.12 for the  $\text{Ni}^{+2}$  complex is also consistent with the octahedral geometry (Patel *et al.*, 2005).

Ultraviolet spectrum of the  $\text{Cu}^{+2}$  complex displays two prominent bands at  $25941 \text{ cm}^{-1}$  and  $13714 \text{ cm}^{-1}$  corresponding to  ${}^2\text{B}_{1g} \rightarrow {}^2\text{A}_{1g}$  and  ${}^2\text{B}_{1g} \rightarrow {}^2\text{E}_{1g}$  transitions supporting tetrahedral geometry around the  $\text{Cu}^{+2}$  ion (Patel *et al.*, 2005). The  $\text{Cu}^{+2}$  complex showed magnetic moment of 1.82 BM which is slightly higher than the expected spin-only value of 1.73 BM for one unpaired electron and offers possibility for tetrahedral geometry of  $\text{Cu}^{+2}$  complexes.

Analytical data and molar conductance values for  $\text{Zn}^{+2}$  complex sufficiently supports the tetrahedral geometry for  $\text{Zn}^{+2}$  complex because it is well known that the  $\text{Zn}^{+2}$  generally forms tetrahedral complexes because of its  $d^{10}$  electronic configuration. The absorption bands at  $28145 \text{ cm}^{-1}$  can be considered in association with intra-ligand transitions only. There were no  $d-d$  transitions seen in the visible spectrum of the  $\text{Zn}^{+2}$  complex and it was found to be diamagnetic in nature.

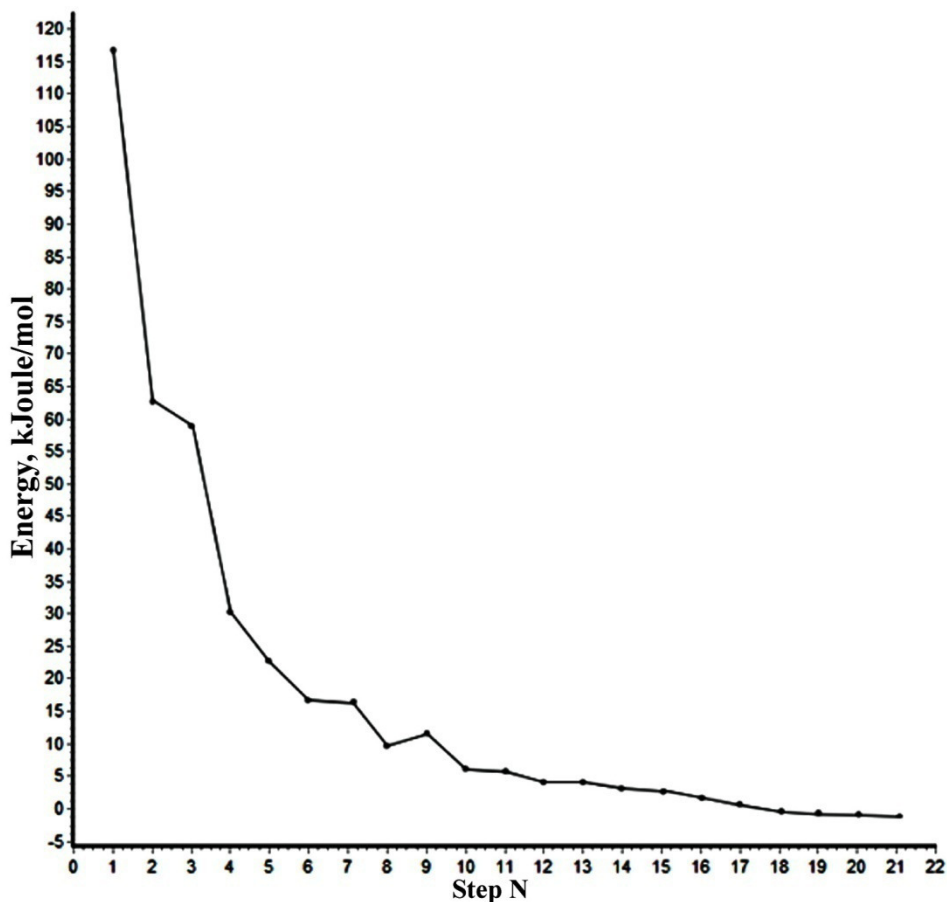


Fig. 4. Optimization steps for PM3 optimization calculations



**Molecular Modeling Studies:** Since the single crystal structure of the ligand compound was not available, molecular mechanics and quantum chemical calculations were used to find the optimized geometries of ligand and metal complexes. Schiff base ligand was initially modeled in ArgusLab 4.0.1 program and Merck Force Field (MMFF94) was used for initial geometry cleanup. A semi empirical PM3 geometry optimization was performed using GAMESS software package. The optimization process went readily to reach to a local minimum. Molecular mechanics was used in the modeling of metal complexes due to their large sizes and sufficient spectral evidences for their structure elucidations. Results of the molecular modeling were visualized by ChemCraft software program version 1.6 (Zhurko & Zhurko, 2005). This program was also used to draw high resolution images of computed molecular models. *Fig. 4* shows the convergence graph of PM3 calculations and *Fig. 5* shows the optimized structure of the ligand.

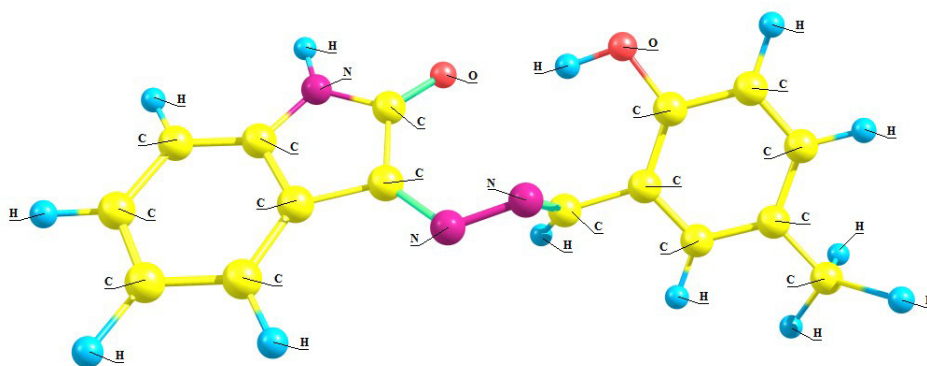


Fig. 5. Optimized geometry of the ligand

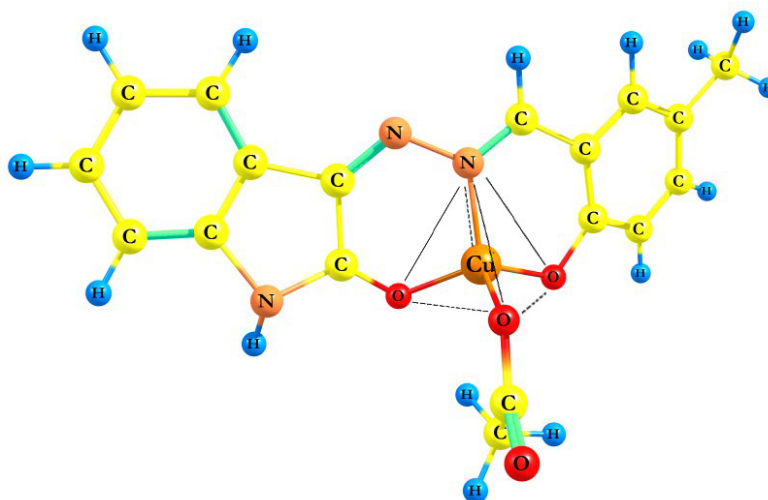


Fig. 6. Optimized geometry of  $\text{Cu}^{+2}$  complex

Optimized structures of metal complexes also supported the tetrahedral geometry for [Cu(Inh)(OAc)] and distorted tetrahedral geometry for [Zn(Inh)(OAc)] and octahedral geometries for [Co(Inh)<sub>2</sub>] and [Ni(Inh)<sub>2</sub>] metal complexes. Fig. 6 - Fig. 9 shows the optimized geometries of the metal complexes.

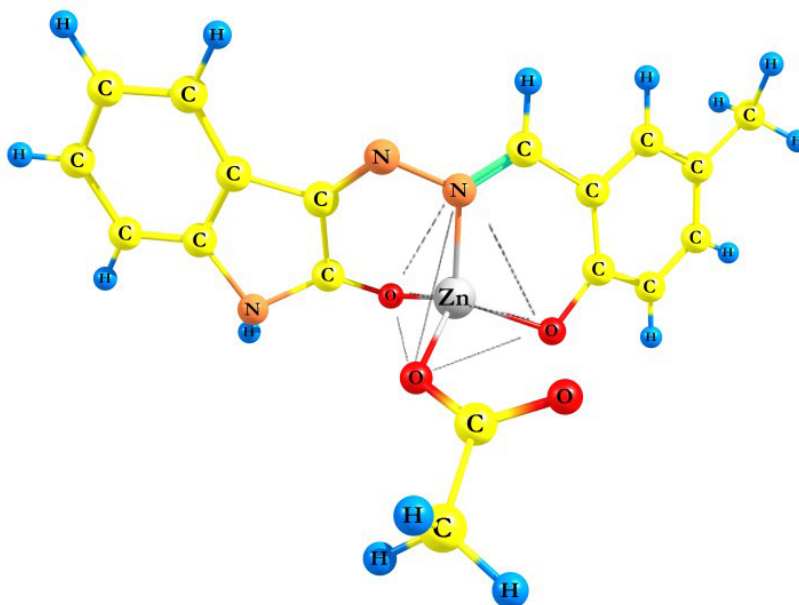


Fig. 7. Optimized geometry of Zn<sup>+2</sup> complex

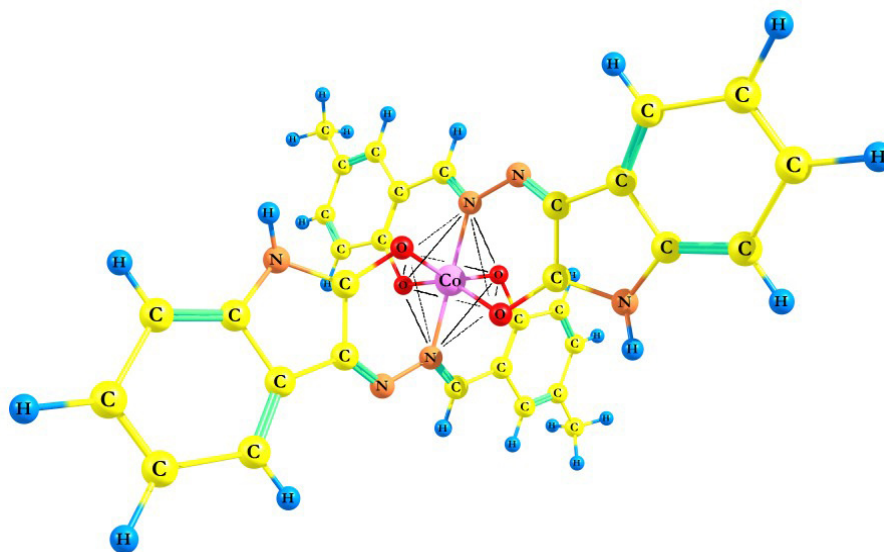


Fig. 8. Optimized geometry of Co<sup>+2</sup> complex

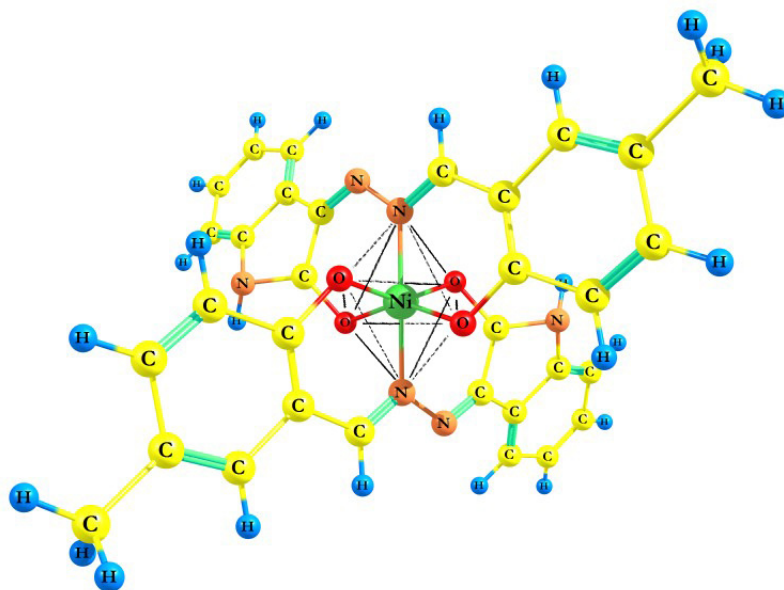
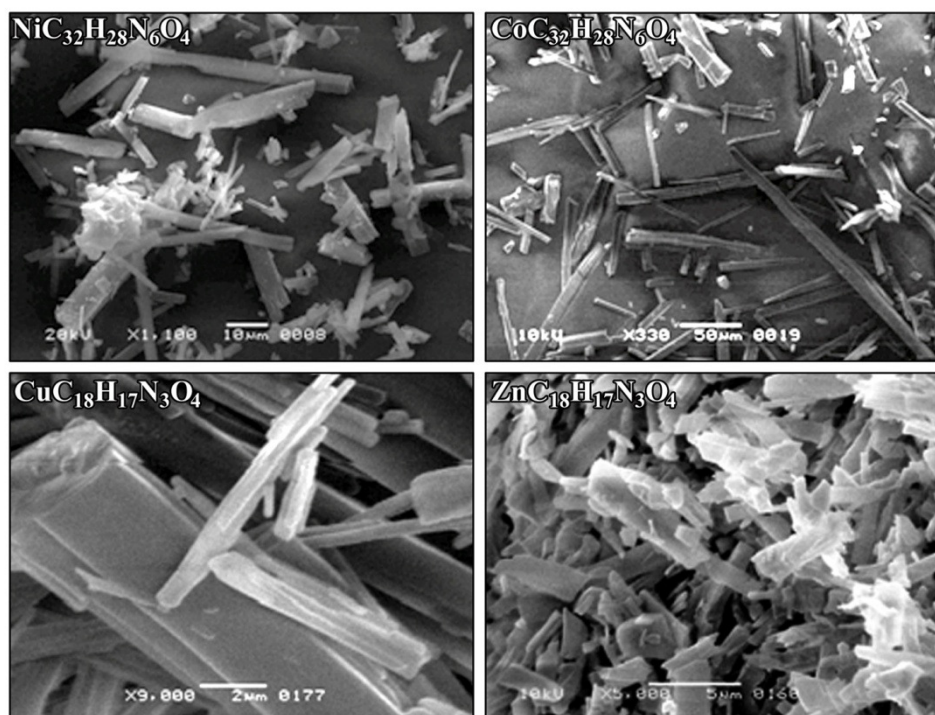
Fig. 9. Optimized geometry of Ni<sup>2+</sup> complex

Fig. 10. SEM Images of Complexes

**SEM Analysis:** Scanning electron microscopy analysis revealed that all complexes have crystalline structures. Crystals are very clear and have sharp edges. The surface of the  $Zn^{+2}$  complex looks bumpy and rough while the surfaces of  $Cu^{+2}$ ,  $Co^{+2}$  and  $Ni^{+2}$  complexes appears glass-smooth with depicted specular highlights from electron beam. Fig. 10 shows the scanning electron micrographs of the complexes.

**Anti Cyanobacterial Activity:** Anti Cyanobacterial Activity data for ligand and its complexes is presented in the Table 4. The increase in the activity of the metal complexes can be explained on the ground of chelation theory (Gudasi, Patil, Vadavi, 2008) since it is well known that polarity of the metal ion is reduced with chelation which can increase the interactions of the metal ion with the constituents of cell wall hence interrupting normal cell functions. Nearly all complexes showed better growth inhibition than the Schiff base ligand. The  $Ni^{+2}$  complex showed total growth inhibition while the rest showed some trace growth of algae over the testing period.

**Table 4. Anti Cyanobacterial Activity Data**

Compounds	Weekly Cyanobacterial Growth Record								
	<i>Lyngbya contorta</i>			<i>Pseudoanabaena lonchoides</i>			<i>Spirulina major</i>		
	Week 1	Week 3	Week 6	Week 1	Week 3	Week 6	Week 1	Week 3	Week 6
<b>HI<sub>nh</sub></b>	trace	light	medium	trace	light	medium	trace	light	medium
[ Co (Inh) <sub>2</sub> ]	nil	trace	trace	nil	nil	trace	nil	nil	trace
[ Ni (Inh) <sub>2</sub> ]	nil	nil	nil	nil	nil	nil	nil	nil	nil
[ Cu (Inh)(OAc) ]	nil	trace	light	trace	light	medium	nil	trace	trace
[ Zn (Inh)(OAc) ]	nil	nil	trace	nil	light	light	nil	nil	trace

**Conclusion:** In this study four new complexes of a Schiff base i.e. “2-hydroxy-5-methylbenzaldehyde-N- (2-oxo-1,2-dihydro-3H-indol-3-ylidene) hydrazone” with  $Co^{+2}$ ,  $Ni^{+2}$ ,  $Cu^{+2}$  and  $Zn^{+2}$  were synthesized, characterized and were screened for their anti-algal activities. Molecular modeling study was performed. Images of the 3D models of the molecules were rendered and all optimized geometries were found well in agreement with spectroscopic characterizations. It was found that for all of the complexes, Schiff

base ligand coordinated with the metal center in a tridentate fashion. In the case of anti-algal activity, the metal complexes were found more potent than the ligand.

## REFERENCES

- ASTM D5589-97. 2002. Standard Test Method for Determining the Resistance of Paint Films and Related Coatings to Algal Defacement, ASTM International, West Conshohocken, PA, 1997.
- Bravo, R.H., V.C. Sylvia, and W. Lazo. 1997. Antimicrobial activity of natural 2-benzoxazolinones and related derivatives, *J. Agri. Food Chem.* 45(8): 3255-3257.
- El-Tabl, A.S., F.A. El-Saied and A.N. Al-Hakimi. 2008. Spectroscopic characterization and biological activity of metal complexes with an ONO trifunctionalized hydrazone ligand. *J. Coordinat. Chem.* 61(15): 2380-2401.
- Gudasi, K.B., M.S. Patil and R.S. Vadavi. 2008. Synthesis, characterization of copper (II), cobalt (II), nickel (II), zinc (II) and cadmium (II) complexes of [7-hydroxy-4-methyl-8-coumarinyl] glycine and a comparative study of their microbial activities. *Euro. J. Medici. Chem.* 43(11): 2436-2441.
- Halgren, T.A. 1999. MMFF VII. Characterization of MMFF94, MMFF94s, and other widely available force fields for conformational energies and for intermolecular-interaction energies and geometries. *J. computat. chem.* 20(7): 730-748.
- Hallegraeff, G.M. 1993. A review of harmful algal blooms and their apparent global increase. *Phycologia.* 32(2): 79-99.
- Khan, K.M., M. Khan, M. Ali, M. Taha, S. Rasheed, S. Perveen and M.I. Choudhary. 2009. Synthesis of bis-Schiff bases of isatins and their antiglycation activity. *Bioorg. Medici. Chem.* 17(22): 7795-7801.
- Landsberg, J.H. 2002. The effects of harmful algal blooms on aquatic organisms. *Reviews in Fisheries Science.* 10(2): 113-390.
- Ouellette, A.J., S.M. Handy and S.W. Wilhelm. 2006. Toxic Microcystis is widespread in Lake Erie: PCR detection of toxin genes and molecular characterization of associated cyanobacterial communities. *Microbial ecology*, 51(2): 154-165.
- Patel, N.H., H.M. Parekh and M.N. Patel. 2005. Synthesis, characterization and biological evaluation of manganese (II), cobalt (II), nickel (II), copper (II), and cadmium (II) complexes with monobasic (NO) and neutral (NN) Schiff bases. *Transit. metal chem.* 30(1): 13-17
- Schmidt, M.W., K.K. Baldrige, J.A. Boatz, S.T. Elbert, M.S. Gordon, J.H. Jensen and S. Su. 1993. General atomic and molecular electronic structure system. *J. computat. chem.* 14(11): 1347-1363.
- Thompson, M.A. 2004. Argus Lab 4.0. 1. *Planaria Software LLC, Seattle, WA.*
- Varghese, S. and M. Muraleedharan Nair. 2010. Antibacterial and antialgal studies of some lanthanide Schiff base complexes. *Int J Appl Bio Pharm Tech.* 2: 608-614.
- Zhurko, G., and D. Zhurko. 2005. ChemCraft: Tool for treatment of chemical data. *Lite version build*, 8, 2005.